THE ASTROPHYSICAL JOURNAL, 381:79–84, 1991 November 1

THE STARBURST RING AROUND THE SEYFERT NUCLEUS IN NGC 7469

A. S. WILSON AND T. T. HELFER
Astronomy Program, University of Maryland, College Park, MD 20742
C. A. HANIFF
105-24 Robinson Laboratory, California Institute of Technology, Pasadena, CA 91125
AND
M. J. WARD
Department of Physics, Nuclear Physics Laboratory, University of Oxford, Keble Road, Oxford OX1 3RH, England, UK
Received 1991 February 11; accepted 1991 April 29

ABSTRACT

We present high-resolution radio continuum, optical emission line, and optical continuum images of the luminous ($\sim 3 \times 10^{11}\ L_\odot$) Seyfert plus circumnuclear starburst hybrid galaxy NGC 7469. The radio images reveal a compact (0".1–0".2 ~ 30–60 pc) source associated with the Seyfert nucleus plus a broken ring of emission centered on it with diameter 3" ($\simeq 1.0$ kpc), both these radio components being nonthermal in origin. The distribution of the flux ratio [O III]λ5007/Hα + [N II]$\lambda\lambda$6548, 6584 over the central 3 kpc reflects a mixture of Seyfert- and H II region-like excited gas. The present images and a recent speckle masking image by Hofmann, Mauder, & Weigelt reveal optical continuum features associated with the radio ring. We suggest that the starburst ring in NGC 7469 has resulted from a gas ring formed through bar-forcing at a dynamical (probably inner Lindblad) resonance. Current starburst models can account for both the far infrared and the nonthermal radio emission if the supernova rate is ~ 1 per year. Models in which Seyfert nuclei are fueled through inflow of gas associated with bar- or oval distortion-driven resonances, on scales ranging from galaxy wide (tens of kpc) to circumnuclear (< 500 pc), are supported by these results. The putative stellar bar and individual supernovae in the ring may be detectable through high-resolution, near-infrared imaging.

Subject headings: galaxies: individual (NGC 7469) — galaxies: nuclei — galaxies: Seyfert — radio sources: galaxies — stars: formation

1. INTRODUCTION

A major problem for black hole models of active nuclei concerns the process by which the material to be accreted ("fuel") is channeled into the environment of the hole. Given the typical accretion rates of 1–100 $M_\odot\ \mathrm{yr}^{-1}$, an attractive source of material is the gas in the host galaxy. However, this gas has considerable angular momentum, nearly all of which must be lost if it is to fall from galaxy-wide dimensions (tens of kpc) to the environment of the hole (hundreds of gravitational radii), where viscosity can take over the outward transport of angular momentum. Various ways in which gas might be forced into the center have been suggested. Tidal effects of companion galaxies may trigger inward mass motions (Toomre & Toomre 1972). Alternatively, gas may be forced toward the center via large scale, nonaxisymmetric components of the gravitational potential in an isolated host galaxy (Simkin, Su, & Schwarz 1980), However, as discussed by Shlosman, Frank, & Begelman (1989), inflow driven by a barlike perturbation slows down at a radius of about one-tenth of the radius of the bar. These authors argued in favor of a "nested bars" scenario, in which bars on successively smaller scales force gas inward.

These processes, suggested for fueling an active nucleus, are also precisely those expected to compress gas clouds and trigger bursts of star formation (e.g., Shu, Adams, & Lizano 1987). Investigation of the nature and structure of starbursts in galaxies also hosting nuclear activity may then provide clues to the mechanism(s) by which both forms of activity are triggered especially in cases where the starburst is very close to the nucleus.

NGC 7469 is a well-known type 1 Seyfert galaxy (e.g., Anderson 1970) with Hubble type (R')SAB(rs)a and heliocentric recession velocity $cz = 4917\ \mathrm{km\ s}^{-1}$. Evidence for the presence of a considerable number of hot stars around its nucleus was first adduced by Cutri et al. (1984). These authors found that nearly 80% of the luminosity in the 3.3 μm dust emission feature arises in a region between 1" (330 pc, assuming $H_0 = 75\ \mathrm{km\ s}^{-1}\ \mathrm{Mpc}^{-1}$) and 3" (1.0 kpc) from the central source and that the dust in this region has a temperature of 300 K or greater. Cutri et al. (1984) argued that neither the continuum source in the Seyfert nucleus nor the radiation from the broad- and narrow-line clouds is capable of heating grains to such high temperatures. Their conclusion was that the dust heating is most likely due to radiation from hot young stars in circumnuclear H II regions. NGC 7469 also exhibits the unidentified emission features in its 8-13 μm spectrum (Aitken, Roche, & Phillips 1981), which is most unusual for a Seyfert galaxy but common for starbursts. Wilson et al. (1986, hereafter WBSW) reported mapping of several optical emission lines in the circumnuclear region of NGC 7469 using long-slit spectroscopy. In addition to the spatially unresolved broad line region, two blended components of emission-line gas, extending over $\simeq 10"$ ($\simeq 3$ kpc), were found. One is of high excitation, exhibits broad lines, has kinematics dominated by radial motions, and is apparently ionized by the Seyfert nucleus. The other component is of low-excitation, exhibits narrow lines, follows normal rotational motion, and is presumably ionized by hot stars. WBSW also noted that the spectrum of the luminous ($\simeq 3 \times 10^{11}\ L_\odot$) mid- and far-infrared source seen by *IRAS* is typical of galaxies with nuclear H II regions

and differs from most Seyfert galaxies, supporting the notion that this emission originates in dust heated by hot stars, not the Seyfert nucleus. Strong emission in the ^{12}CO $J = 1$–0 (Sanders et al. 1988; Meixner et al. 1990) and in the H_2 $v = 1$–0 S(1) (Heckman et al. 1986) lines from the region within a few arcseconds of the nucleus provides unambiguous evidence for a concentration of molecular gas; Meixner et al. (1990) find 1–2×10^{10} $M_\odot$ of molecular gas within a 2.5 kpc radius of the nucleus. Also, the 8″ (2.6 kpc) diameter "diffuse" radio continuum source (Ulvestad, Wilson, & Sramek 1981; Condon et al. 1982) is probably fueled by the starburst.

These observations provide conclusive evidence for a circumnuclear starburst in NGC 7469, but give little information about its detailed structure. In the present paper, we report high-resolution radio continuum observations that resolve the "diffuse" radio continuum source into a circumnuclear ring (§ 3.1). New high-resolution optical images are also consistent with a ringlike morphology for the low-excitation gas and the continuum emission near the nucleus (§ 3.2). In § 4, we review the many similarities between the disks of NGC 7469 and NGC 1068, comment on the applicability of current starburst models to NGC 7469, and discuss the origin of the ring and its relevance to the problem of fueling active galactic nuclei.

2. OBSERVATIONS AND DATA REDUCTION

2.1. *Radio Observations*

NGC 7469 was observed in 1989 January for 2.5 hr at 6 cm (4.9 GHz) and 4 hr at 2 cm (15.0 GHz) with the Very Large Array[1] in "A" configuration, giving resolutions (FWHM) of 0.″38 at 6 cm and 0.″12 at 2 cm. 2251+158 was used as the phase and amplitude calibrator, 3C138 set the zero of polarization angle, and 3C 48 and 286 were observed to set the absolute flux scale. Data reduction followed standard procedures, including self calibration at 6 cm.

2.2. *Optical Observations*

Optical imaging observations of NGC 7469 were obtained on 1986 September 24 and 25 with the University of Hawaii's 88 inch (2.2 m) telescope. The Cambridge GEC 576 × 385 pixel CCD was used at the f/10 Cassegrain focus, giving a pixel size of 0.″197. Exposures were made through filters with center wavelengths (Å)/bandwidths (Å) of 5120/90, 5260/110, 6690/150, and 6430/90, which provided "on-band" and "off-band" images for [O III]λ5007 and "on-band" and "off-band" images for Hα + [N II]λλ6548, 6584, respectively. [O III]λ5007 is redshifted to ≃5089 Å, which is near the half-peak intensity transmission point of the 5120/90 filter. Because of the rapidly changing transmission with wavelength in this region of the filter's passband, line emission which is Doppler shifted blueward w.r.t. systemic is observed with somewhat reduced sensitivity compared with line emission Doppler-shifted redward. Using the velocity field of the *peaks* of [O III]λ5007 given by WBSW and the known transmission curve of the filter, we estimate this change of transmission over the nebulosity at a maximum of 7%. Gas in the faint blue *wings* of [O III]λ5007 may be attenuated by up to 30% compared with gas near systemic. The 6690/150 filter includes almost all of the broad Hα emission and all of narrow Hα and [N II]λλ6548, 6584. Although the lines [O I]λλ6300, 6363 are included in the Hα + [N II]λλ6548, 6584 "off-band" filter, they are very weak in NGC 7469 (cf. spectra in Morris & Ward 1988 and Wilson & Nath 1990) and should not significantly affect the continuum image.

Data reduction followed the procedures described in Haniff, Wilson, & Ward (1988). Two stars were included in all frames and were used to align the "on-" and "off-band" images prior to subtraction of the latter from the former, to give an image in the emission line. Smoothing of either the "off-band" or the "on-band" was performed to ensure the same spatial resolution before these subtractions, resulting in resolutions (FWHM) of 1.″1 for the [O III]λ5007 image and 0.″9 for the Hα + [N II]λλ6548, 6584 image. Absolute flux calibrations of the emission-line images were obtained by scaling the observed counts such that the integrated [O III]λ5007 and Hα + [N II]λλ6548, 6584 fluxes in a 10″ diameter circular region centered on the nucleus were 7.7×10^{-13} and 4.3×10^{-12} ergs cm^{-2} s^{-1}, respectively (Anderson 1970; Wampler 1971; Yee 1980). This procedure should be reliable for [O III]λ5007 but assumes that the broad component of Hα has not varied since the absolute flux measurements were made. After smoothing the Hα + [N II]λλ6548, 6584 image to 1.″1 resolution, a map of the flux ratio $F_{[O\,III]\lambda5007}/F_{H\alpha+[N\,II]\lambda\lambda6548,6584}$ was obtained by direct division. Because of the uncertainty in the Hα + [N II]λλ6548, 6584 flux calibration noted above, the *absolute* values in this ratio map should be treated with caution. *Variations* in the flux ratio are more reliable, but are subject to the attenuation of blueshifted [O III]λ5007 emission noted above.

3. RESULTS

3.1. *Radio Maps*

The 6 cm radio map, shown as a contour map in Figure 1 and as a radiograph in Figure 2 (Plate 2), is dominated by a strong compact source coincident with the Seyfert nucleus (Table 1). This source is extended by ≃0.″2 (66 pc) in P.A. ≃ 101° on the 6 cm map and by ≃0.″1 (33 pc) in P.A.

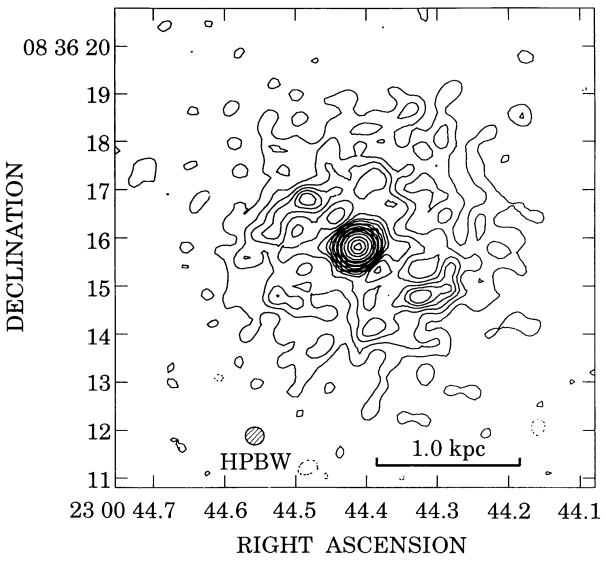

FIG. 1.—VLA image of the 6 cm brightness distribution in the central parts of NGC 7469 with beam 0.″39 × 0.″37 (FWHM) in P.A. 108°. Contours are plotted at −0.5, 0.5, 1, 1.5, 2, 2.5, 3, 4, 5, 7.5, 10, 15, 20, 30, 50, 70, and 90% of the peak brightness of 18.0 mJy (beam area)$^{-1}$.

[1] The Very Large Array is a facility of the National Radio Astronomy Observatory, which is operated by Associated Universities Inc., under contract with the National Science Foundation.

PLATE 2

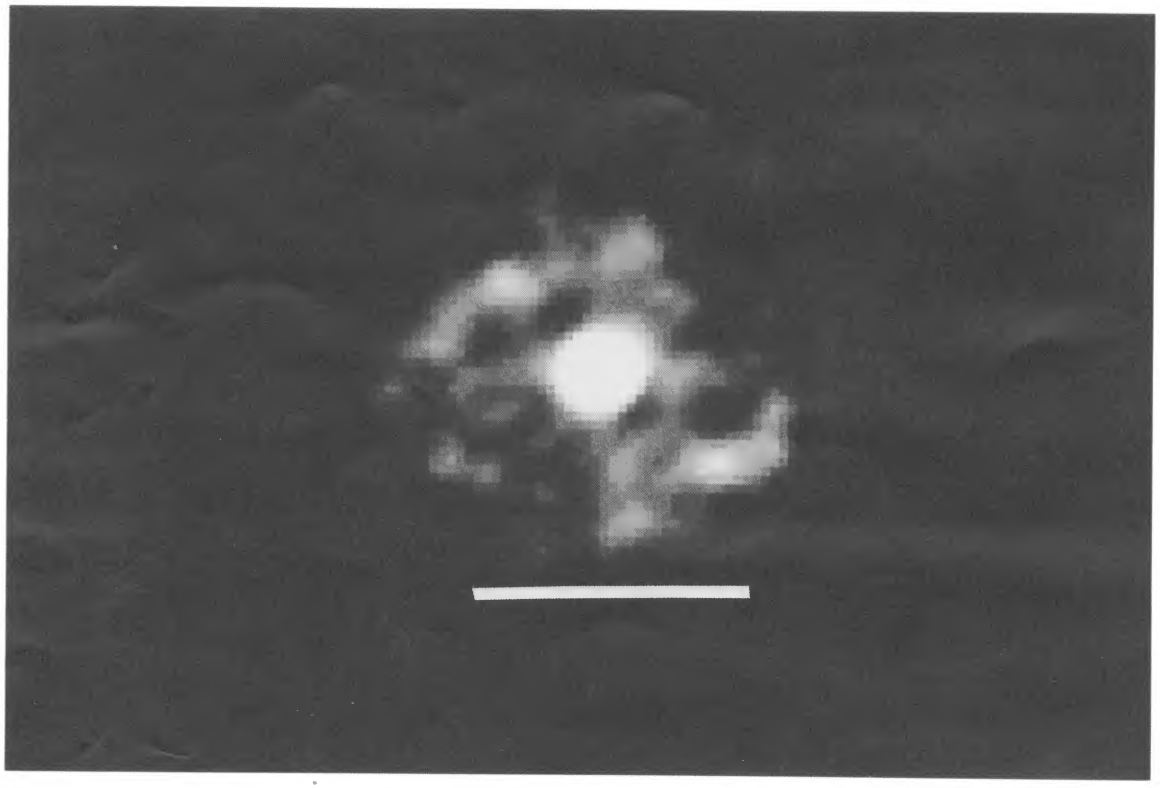

FIG. 2.—A radiograph of the 6 cm VLA image which is shown as a contour map in Fig. 1. The white bar is 3″ (1.0 kpc) long.

WILSON, HELFER, HANIF, & WARD (see 381, 80)

TABLE 1

RADIO FLUXES (in mJy) FROM THE CENTRAL REGION OF NGC 7469

Frequency (GHz)	Nuclear Source	Total Emission within 5″ of Nucleus
2.7.....	...	113 ± 6[a]
4.9.....	21.2 ± 1[b]	65 ± 3[c]
15.0.....	8.0 ± 0.8[b]	...

[a] From Condon & Dressel 1978.

[b] Total flux of nuclear source as observed with a 0.″4 beam. At the full resolution of the 15.0 GHz map, the peak nuclear flux is 4.3 mJy.

[c] From Ulvestad, Wilson, & Sramek 1981.

$\simeq 85°$ on the 2 cm map. Its spectral index, $\alpha_2^6 = 0.87 \pm 0.05$ ($S \propto \nu^{-\alpha}$), is indicative of optically thin synchrotron radiation. This nuclear radio source is unpolarized at 6 cm (< 1%).

The 8″ (2.6 kpc) radio "halo" previously observed by Ulvestad, Wilson, & Sramek (1981) and Condon et al. (1982) is well resolved by the new 6 cm observation. It is clear that much of this halo emission is confined to an annular structure of diameter $\simeq 3''$ (1.0 kpc) centered on the nucleus (Figs. 1 and 2). This ring is of somewhat irregular brightness, being brightest to the NE and SW of the nucleus and showing a gap to the NW. The total halo flux density at 6 cm is 43.8 ± 4 mJy (Table 1) and, assuming power-law spectra between 11 and 2 cm for both nuclear source and halo, the halo spectral index is $\alpha_2^{11} = 0.95 \pm 0.1$. A nonthermal radio spectrum for the ring is also indicated by the upper limits on its brightness obtained directly from our 2 cm observations.

3.2. *Optical Maps*

Our continuum-subtracted emission line images in [O III] λ5007 and Hα + [N II]λλ6548, 6584 are shown in Figures 3*a* and 3*b*, respectively. In common with previously published lower resolution images (Heckman et al. 1986), they show extended ($\simeq 10'' = 3.3$ kpc diameter in Hα + [N II]λλ6548, 6584) emission around a bright peak, which coincides with the maximum of continuum light to <0.″1 (<30 pc). The [O III]λ5007 emission is much more centrally concentrated than the Hα, but shows a plume of gas extending to the north, which is less prominent in Hα. The spatial resolution is not good enough to separate cleanly the nucleus from any emission-line counterpart to the radio ring. However, computation of the flux ratio map $R = F_{[\mathrm{O\ III}]\lambda 5007}/F_{\mathrm{H}\alpha+[\mathrm{N\ II}]\lambda\lambda 6548,6584}$ (Fig. 3*c*) provides a measure of the excitation of the gas which may, in principle, be used to distinguish Seyfert excited gas from "normal" H II regions. In practice, the interpretation of the distribution of R is complicated by a number of factors, each of which will tend to reduce R below the range of $F_{[\mathrm{O\ III}]\lambda 5007}/F_{\mathrm{H}\alpha} \simeq 1$–5 expected for an unreddened,

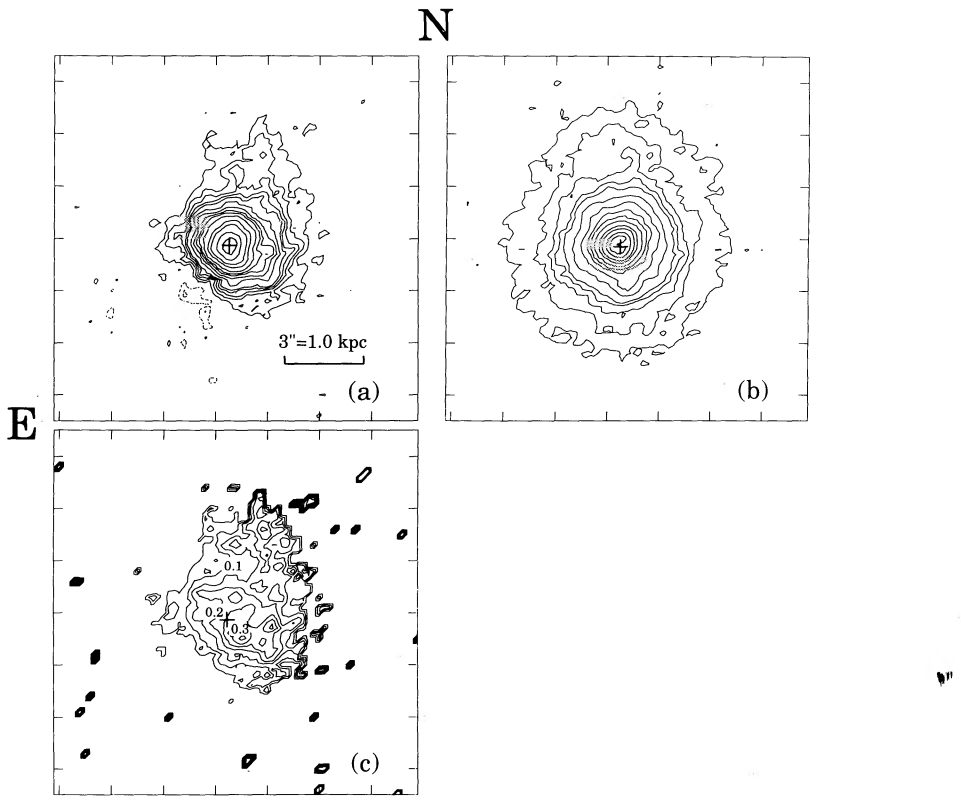

FIG. 3.—Optical emission line and line ratio distributions in the central part of NGC 7469. The cross marks the peak of continuum light. The ticks on the border are separated by 2.″0 (10 pixels). (*a*) [O III]λ5007. Contours are plotted at −2, −1, 1, 2, 3, 4, 5, 7.5, 10, 12.5, 15, 20, 30, 40, 60 and 80% of the peak brightness of 3.0×10^{-13} ergs cm^{-2} s^{-1} (arc sec)$^{-2}$. (*b*) Hα + [N II]λλ6548, 6584. Contours are plotted at −1, 1, 2, 3, 4, 5, 7.5, 10, 12.5, 15, 20, 30, 40, 60, and 80% of the peak brightness of 1.3×10^{-12} ergs cm^{-2} s^{-1} (arc sec)$^{-2}$. The "pacman" shape of the top contour is not real but results from 2 pixels of reduced sensitivity. (*c*) The result of dividing the [O III]λ5007 map by the Hα + [N II]λλ6548, 6584 map at locations where the brightness is >3 times rms noise in both maps. Because of the possibility of systematic errors in the fluxes the relative variations over this map are more reliable than the absolute values.

typical power-law photoionized, narrow-line region. The inclusion of the strong broad-line Hα emission in our filter greatly reduces R right at the nucleus. Also, R is reduced by reddening and by the inclusion of [N II]λλ6548, 6584 in the filter passband. Bearing these caveats in mind, we note that R drops from peak values of $\simeq 0.4$ near and just to the west of the nucleus to <0.1 some 1″–2″ (330–660 pc) away, except to the N and NW, where R remains greater than 0.1. We see evidence, therefore, for an increasing contribution to the emission lines from H II regions at increasing distance from the nucleus, as already inferred by WBSW from the much less ambiguous ratio $F_{[O\,III]\lambda 5007}/F_{H\beta}$.

The red continuum (Hα "off-band") image with 0.″9 resolution (Fig. 4*a*) shows a "lumpy" structure within 2″ (660 pc) of the nucleus, some of which has already been noticed by Barbieri, di Serego Alighieri, & Zambon (1977). This structure may be seen more clearly in Figure 4*b*, which shows the red continuum image after subtraction of $\simeq 75\%$ of the flux of the nuclear point source. The point spread function used for this subtraction was obtained from one of the stars in the field. The most prominent "lumps" are found $\simeq 1.''5$ (500 pc) from the nucleus in P.A.'s $\simeq 40°$ and 245°. A much higher resolution red continuum image has been obtained by Hofmann, Mauder, & Weigelt (1989) using speckle masking techniques and is reproduced here as Figure 4*c*. An excellent correspondence is found between the "lumps" in the direct image and the off-nuclear peaks in the speckle map. The speckle image shows that the circumnuclear structure forms an irregular ring of diameter 3″ (1 kpc), the same as the radio ring (Fig. 4*d*). Some detailed coincidences are found between optical and radio continuum features, e.g., the radio peak 1.″5 NE (P.A. 47°) of the nucleus shows up strongly in the speckle map. This similarity of radio and optical continuum distributions suggests that the circumnuclear optical continuum emission represents direct emission from hot stars in the ring.

Recently, Keto et al. (1991) have obtained a 12.5 μm mid infrared image of NGC 7469 with $\simeq 1''$ resolution. Their map shows an elongated distribution of emission, extending 3″ (1.0 kpc) in P.A. 78°. Comparison with the radio map (Figs. 1 and 2) suggests the mid-infrared image represents emission from the nucleus plus the two brightest features in the radio ring (P.A.'s $\simeq 70°$ and 250° w.r.t. the nucleus), blurred together by the lower resolution of the 12.5 μm picture. This off-nuclear mid-infrared emission might then be understood in terms of dust heated by hot stars in the brightest part of the starburst ring.

4. DISCUSSION

4.1. *Circumnuclear Starburst*

The morphology of the extended radio emission shown in Figures 1 and 2 is unlike most Seyfert nuclei which, when spatially resolved, tend to show "linear" (i.e., double triple, or jetlike) structures powered by the active nucleus. Furthermore, the ratio $u = \log (S_{60\mu m}/S_{1.4\,GHz}) = 2.11$ (for the integrated radio emission) or 2.27 (for the halo radio emission only), both of which are typical of "starburst" regions (e.g., Condon &

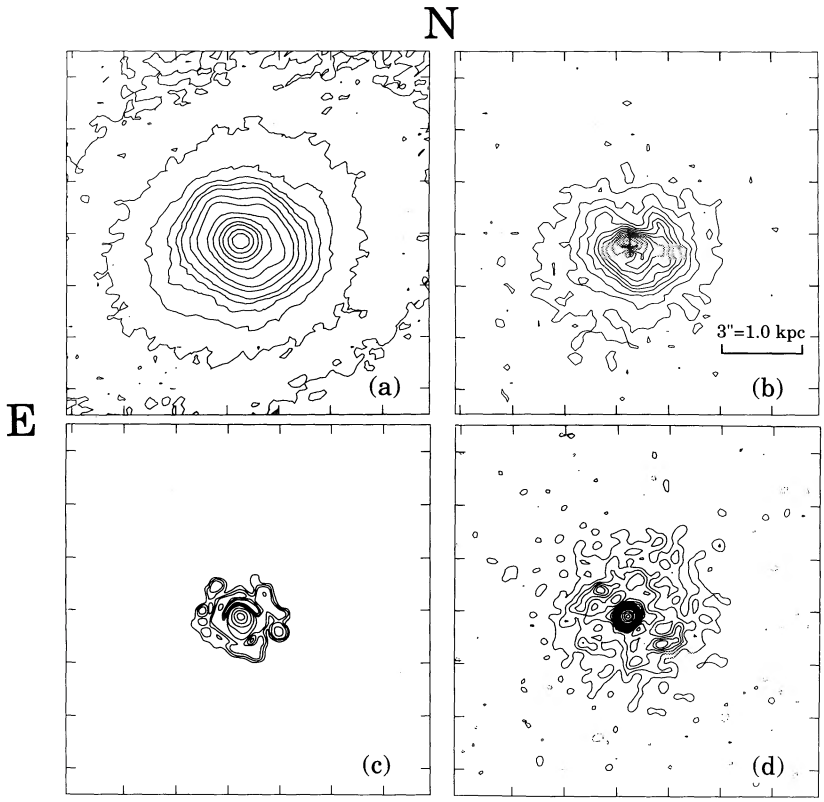

FIG. 4.—Optical and radio continuum distributions in the central part of NGC 7469. The ticks on the border are separated by 2.″0 (10 pixels). (*a*) Red (6430 Å) continuum. Contours are plotted at −0.5, 0.5, 1, 2, 3, 4, 5, 7.5, 10, 15, 20, 30, 40, 60, and 80% of the peak. (*b*) The result of subtracting, at the nucleus (*the cross*), a point spread function with 75% of the peak flux from the red continuum image shown in (*a*). Contours are plotted at equal increments of 7.5% from 7.5% to 90% of the peak brightness of this (i.e., the p.s.f. subtracted) map. (*c*) Red (6100 Å) continuum obtained by speckle masking techniques (from Hofmann, Mauder, & Weigelt 1989). (*d*) Radio continuum (see Fig. 1).

Broderick 1988), as are the *IRAS* colors (e.g., WBSW). Also, the emission line morphologies (Fig. 3) are unlike the aligned narrow-line regions often found in Seyfert galaxies (e.g., Whittle et al. 1988; Haniff, Wilson, & Ward 1988) and the line ratios suggest that much of the off-nuclear gas is ionized by hot stars. The radio map indicates that much of the star formation is occurring in a ring of diameter 1.0 kpc centered on the Seyfert nucleus. As a caveat, we note that the highest excitation line emission (Fig. 3*c*) seems to align in P.A. $\approx 240°$, which is roughly the axis (P.A. $\simeq 50°$–$230°$) joining the two brightest off-nuclear radio peaks, suggesting that *some* of the radio emission at these peaks *might* be fueled by nuclear ejection. The compact nuclear radio source has a radio power $P_{4.9\,\mathrm{GHz}} = 1.2 \times 10^{22}$ WHz^{-1} and a size of $\simeq 30$–60 pc, properties typical of the nuclei of type 1 Seyfert galaxies (e.g., Ulvestad & Wilson 1984).

4.2. *Comparison with NGC 1068*

A comparison of the disks of NGC 1068 and NGC 7469 is presented in Table 2. A strong similarity is apparent in almost all observed properties.

Although NGC 1068 is classified SA (based on optical plates), near-infrared images reveal an inner bar (Scoville et al. 1988; Thronson et al. 1989), and kinematic studies show the disk is heavily ovally distorted (Baldwin, Wilson, & Whittle 1987). The mid- and far-infrared spectral indices (α) given for NGC 1068 in Table 2 refer to the disk alone and exclude emission from the nucleus (Telesco et al. 1984). For NGC 7469, such a direct separation is not possible and the values of α refer to the integrated emission. In any case, the steep spectrum of each galaxy between 25 and 60 μm and the flatter one between 60 and 100 μm are tpical of galaxies with nuclear H II region emission-line spectra, suggesting the emission in these wavebands is dominated by dust heated by hot stars. For this reason, the values of L_{ir}, which were calculated from the 60 and 100 μm fluxes, have not been corrected for any nuclear contribution. The radio powers are for the disk alone. An intriguing similarity between NGC 1068 and NGC 7469 is the presence of *both* inner and outer rings of similar linear diameter. This aspect will be discussed more fully in § 4.4.

TABLE 2

A COMPARISON OF THE DISKS OF NGC 1068 AND NGC 7469

Parameter	NGC 1068	NGC 7469
Assumed Distance (Mpc)	15.1	68.3
Hubble type[a]	(R)SA(rs)b	(R′)SAB(rs)a
$\log L_B (L_\odot)$[b]	10.86	10.92
$\log L_{\mathrm{ir}} (L_\odot)$[c]	10.96	11.41
$\log M_{\mathrm{warmdust}} (M_\odot)$[c]	6.78	7.34
$\log M_{\mathrm{H\,I}} (M_\odot)$[c]	9.45	9.55
$\log M_{\mathrm{H_2}} (M_\odot)$[c]	10.07	10.20
$L_{\mathrm{ir}}/M_{\mathrm{H_2}} (L_\odot/M_\odot)$[c]	7.89	16.09
L_{ir}/L_B	1.3	3.1
$\dot{M}_{\mathrm{OBA}} (M_\odot\ \mathrm{yr}^{-1})$[d]	13	26
τ (yr)[e]	1.2×10^9	7.4×10^8
$\log P_{4.9\,\mathrm{GHz}}$ (WHz^{-1})[f]	22.25	22.39
α_{25}^{60}[g]	1.86	1.78
α_{60}^{100}[g]	0.72 (0.25)	0.45
D_{in} (kpc)[h]	2.1	1.0
D_{out} (kpc)[i]	25	27

[a] From RC2.

[b] Obtained by subtracting the nuclear magnitude in B from the B_T^0 magnitude given in RC2 (de Vaucouleurs, de Vaucouleurs, & Corwin 1976).

[c] From Young et al. 1989 adjusted to the different distances assumed here.

[d] Rate at which gas is converted into O, B, and A stars, under the assumption that they produce most of the luminosity (Scoville & Young 1983).

[e] Gas depletion times $\tau = (M_{\mathrm{H\,I}} + M_{\mathrm{H_2}})/\dot{M}_{\mathrm{OBA}}$.

[f] From Wilson & Ulvestad 1982 for NGC 1068 and this paper for NGC 7469.

[g] Spectral indices α ($S \propto \nu^{-\alpha}$) of the disk between 25 and 60 μm, and between 60 and 100 μm. For NGC 1068, the values given are from the disk spectrum given in Fig. 4 of Telesco, Becklin, & Wynn-Williams 1984, except for the value of α_{60}^{100} in parentheses, which is from the *IRAS* fluxes given by Young et al. 1989. The spectral indices for NGC 7469 are from the *IRAS* fluxes (Young et al. 1989).

[h] Diameters of the inner ring, taken from Myers & Scoville 1987 for NGC 1068 and from this paper for NGC 7469.

[i] Major axis diameters of the outer ring, from the Palomar Sky Survey.

4.3. *Starburst Models*

If the total infrared plus blue luminosity (Table 2) of NGC 7469 is taken as the bolometric luminosity of the starburst, it is possible to estimate the required supernova rate ν. For the nine models listed by Rieke et al. (1980) in their Table 2, the mean ratio $\nu(\mathrm{SN\ yr}^{-1})/L_{\mathrm{bol}}\ (10^{10}\ L_\odot) = 0.029$. We thus expect $\nu \simeq 0.97$ SN yr^{-1} given $L_B + L_{\mathrm{ir}} = 3.4 \times 10^{11}\ L_\odot$.

The most recent discussion of the radio emission from a starburst is that of Condon & Yin (1990). These workers use the ratio of the total nonthermal radio luminosity of our Galaxy to the Galactic Type II supernova rate as a measure of the efficiency with which supernovae produce radio emission in a starburst. For $\nu = 0.97$ SN yr^{-1}, their equation (8) predicts $\log P_{4.9\,\mathrm{GHz}}$ (WHz^{-1}) = 22.55 for NGC 7469, in reasonable agreement with the observed value (Table 2). Thus the bolometric luminosity and radio emission of the circumnuclear disk of NGC 7469 are compatible with a supernova rate of 0.97 yr^{-1}. However, the processes by which radio emission is produced in circumnuclear starbursts are poorly understood. The high concentration of supernovae may lead to overlapping remnants and the high ambient density would be expected to modify the evolution of the synchrotron luminosity. Under these circumstances, ad hoc assumptions about the radio emission per supernova should be treated with caution (cf. Ulvestad 1982), even if they provide estimates of supernova rates compatible with those obtained by other methods.

4.4. *Nature of the Rings*

The favored explanation for rings in galaxies involves dynamical resonances between the orbital motions and the pattern speed of a bar or oval distortion. Models such as those of Schwarz (1981) show how forcing by the bar leads to ringlike concentrations of gas, which give stellar rings after star formation. An extensive study by Buta (1986a) has provided strong observational support for this hypothesis. He argues for identification of outer rings with the outer Lindblad resonance, inner rings with the inner Lindblad resonance or the second harmonic resonance, and nuclear rings with the inner Lindblad resonance. In his study of NGC 1433, which he refers to as the prototype of revised Hubble type (R′)SB(r)ab, Buta (1986b) identifies its three rings with just these three resonances. Star formation is a common feature of rings. Nuclear rings of early to intermediate barred spirals are often found near the turnover radius of the rotation curve, supporting an association with the inner Lindblad resonance (Buta 1987; see also appendix in Kormendy & Norman 1979). Indeed, Telesco & Decher (1988) have argued that the star forming inner ring in

NGC 1068 results from bar-driven density waves at two inner Lindblad resonances.

The nuclear starburst ring in NGC 7469 is probably a similar structure. The turnover radius of the rotation curve of NGC 7469 is 3″–5″ (1.0–1.7 kpc), and curvature is probably present on still smaller scales (De Robertis & Pogge 1986; WBSW). Such a form is consistent with the notion that the nuclear starburst ring is associated with the inner Lindblad resonance. The diameter of the nuclear ring in NGC 7469 is $\simeq 1$ kpc, which is typical of nuclear rings. Subarcsecond resolution, near-infrared measurements could isolate the old stellar population from the starburst and reveal a small-scale ($\simeq 500$ pc) inner bar, analogous to what is found in NGC 1068 (Scoville et al. 1988). The shape, size, and orientation of the ring with respect to such a bar could confirm the inner Lindblad resonance interpretation (e.g., Hummel, van der Hulst, & Keel 1987). This situation would be consistent with the proposal of Simkin, Su, & Schwarz (1980) that the Seyfert phenomenon is fed by gas transported into the nucleus by a bar. Their models showed strong inflow in association with an inner Lindblad resonance; they argued that this inward transport is self sustaining since the continuous pile up of gas increases the central density and maintains (or enhances) the inner Lindblad resonance. Shlosman, Frank, & Begelman (1989) have emphasized the difficulty of transporting material inward to feed the putative black hole from typical galactic scales ($\simeq 10$ kpc) down to the scales of the central accretion disk ($\ll 1$ pc). They propose that the gas which accumulates in the central kpc or so, as a consequence of inflow driven by a large-scale bar, forms a disk which becomes dynamically unstable and forms a gaseous bar, allowing further infall. Our results on NGC 7469 provide support for this suggestion.

While the outer rings in NGC 1068 and NGC 7469 may reflect internal dynamical resonances, they could also represent a density wave driven by interaction with a companion (e.g., Kormendy & Norman 1979). This situation is perhaps more plausible for NGC 7469, which has a physical companion (IC 5283) only 80″ (26 kpc) away (Burbidge, Burbidge, & Prendergast 1963).

5. CONCLUSIONS

The conclusions of this paper are as follows:

1. The radio emission from the circumnuclear starburst in NGC 7469 is largely confined to a ring of diameter 3″ = 1.0 kpc (§ 3.1).

2. There is clear evidence for optical continuum emission and probably optical line emission from the ring (§ 3.2).

3. The disks of NGC 1068 and NGC 7469 exhibit a strong similarity in almost all observed properties (Table 2).

4. Current star formation models can account for the luminous ($2.6 \times 10^{11}\ L_{\odot}$) far infrared emission and the strength of the nonthermal radio emission in NGC 7469, with an expected supernova rate of ~ 1 per year (§ 4.3).

5. The starburst ring is probably a result of concentration of gas into a ring via resonances between orbital motion and a rotating barlike or ovally distorted potential. Such an interpretation also provides support for "bars within bars" models (e.g., Shlosman, Frank, & Begelman 1989), in which Seyfert activity is fueled by forcing of disk gas inwards by nonaxisymmetric gravitational potentials on a hierarchy of scales, ranging from galaxy wide (tens of kpc) to circumnuclear (< 500 pc).

Further support for these conclusions could be provided by the detection of a compact stellar bar and of individual supernovae in the ring (see van Buren & Norman 1989) by means of high spatial resolution imaging in the near-infrared.

We thank NRAO and the University of Hawaii for observing time on the VLA and the University of Hawaii 88 inch telescope. CAH is supported by a NATO/SERC research fellowship. This research was supported by NSF grant AST 8719207 and NASA grant NAG 8-529 to the University of Maryland. Heidi Kirkpatrick and Rob Gruendl assisted with the reduction of the optical data and the production of the radiograph, respectively. A. S. W. is grateful to the Graduate School, University of Maryland for a Faculty Research Fellowship during the completion of this work.

REFERENCES

Aitken, D. K., Roche, P. F., & Phillips, M. M. 1981, MNRAS, 196, 101P
Anderson, K. S. 1970, ApJ, 162, 743
Baldwin, J. A., Wilson, A. S., & Whittle, M. 1987, ApJ, 319, 84
Barbieri, C., di Serego Alighieri, S., & Zambon, M. 1977, A&A, 57, 353
Burbidge, E. M., Burbidge, G. R., & Prendergast, K. H. 1963, ApJ, 137, 1022
Buta, R. J. 1986a, ApJS, 61, 609
———. 1986b, ApJS, 61, 631
———. 1987, ApJS, 64, 1
Clements, E. D. 1981, MNRAS, 197, 829
Condon, J. J., & Broderick, J. J. 1988, AJ, 96, 30
Condon, J. J., Condon, M. A., Gisler, G., & Puschell, J. J. 1982, ApJ, 252, 102
Condon, J. J., & Dressel, L. L. 1978, ApJ, 221, 456
Condon, J. J., & Yin, Q. F. 1990, ApJ, 357, 97
Cutri, R. M., Rudy, R. J., Rieke, G. H., Tokunaga, A. T., & Willner, S. P. 1984, ApJ, 280, 521
De Robertis, M. M., & Pogge, R. W. 1986, AJ, 91, 1026
de Vaucouleurs, G., de Vaucouleurs, A., & Corwin, Jr., H. G. 1976, Second Reference Catalogue of Bright Galaxies (Austin: University of Texas Press)
Haniff, C. A., Wilson, A. S., & Ward, M. J. 1988, ApJ, 334, 104
Heckman, T. M., Beckwith, S., Blitz, L., Skrutskie, M., & Wilson, A. S. 1986, ApJ, 305, 157
Hofmann, K.-H., Mauder, W., & Weigelt, G. 1989, in Proc. ESO Workshop Conf. 32, Extranuclear Activity in Galaxies, ed. E. J. A. Meurs & R. A. E. Fosbury (ESO: Garching bei München), 35
Hummel, E., van der Hulst, J. M., & Keel, W. C. 1987, A&A, 172, 32
Keto, E., Ball, R., Arens, J., Jernigan, G., & Meixner, M. 1991, ApJ submitted
Kormendy, J., & Norman, C. A. 1979, ApJ, 233, 539
Meixner, M., Puchalsky, R., Blitz, L., Wright, M. C. H., & Heckman, T. M. 1990, ApJ, 354, 158
Morris, S. L., & Ward, M. J. 1988, MNRAS, 230, 639
Myers, S. T., & Scoville, N. Z. 1987, ApJ, 312, L39
Rieke, G. H., Lebofsky, M. J., Thompson, R. I., Low, F. J., & Tokunaga, A. T. 1980, ApJ, 238, 24
Sanders, D. B., Scoville, N. Z., Sargent, A. I., & Soifer, B. T. 1988, ApJ, 324, L55
Schwarz, M. P. 1981, ApJ, 247, 77
Scoville, N. Z., Matthews, K., Carico, D. P., & Sanders, D. B. 1988, ApJ, 327, L61
Scoville, N. Z., & Young, J. S., 1983, ApJ, 265, 148
Shlosman, I., Frank, J., & Begelman, M. C. 1989, Nature, 338, 45
Shu, F. H., Adams, F. C., & Lizano, S. 1987, ARAA, 25, 23
Simkin, S. M., Su, H. J., & Schwarz, M. P. 1980, ApJ, 237, 404
Telesco, C. M., Becklin, E. E., Wynn-Williams, C. G., & Harper, D. A. 1984, ApJ, 282, 427
Telesco, C. M., & Decher, R. 1988, ApJ, 334, 573
Thronson, H. A. Jr., et al. 1989, ApJ, 343, 158
Toomre, A., & Toomre, J. 1972, ApJ, 178, 623
Ulvestad, J. S. 1982, ApJ, 259, 96
Ulvestad, J. S., & Wilson, A. S. 1984, ApJ, 278, 544
Ulvestad, J. S., Wilson, A. S., & Sramek, R. A. 1981, ApJ, 247, 419
van Buren, D., & Norman, C. A. 1989, ApJ, 336, L67
Wampler, E. J. 1971, ApJ, 164, 1
Whittle, M., Pedlar, A., Meurs, E. J. A. Unger, S. W., Axon, D. J., & Ward, M. J. 1988, ApJ, 326, 125
Wilson, A. S., Baldwin, J. A., Sun, Sze-Dung, & Wright, A. E., 1986, ApJ, 310, 121 (WBSW)
Wilson, A. S., & Nath, B. 1990, ApJS, 74, 731
Wilson, A. S., & Ulvestad, J. S. 1982, ApJ, 263, 576
Yee, H. K. C. 1980, ApJ, 241, 894
Young, J. S., Xie, S., Kenney, J. D. P., & Rice, W. L. 1989, ApJS, 70, 699